Available online at www.sciencedirect.com
SCIENCE DIRECT®
Remote Sensing of Environment 88 (2003) 423–441
Remote Sensing of Environment
www.elsevier.com/locate/rse

Effects of seasonal hydrologic patterns in south Florida wetlands on radar backscatter measured from ERS-2 SAR imagery

Eric S. Kasischke[a,*], Kevin B. Smith[a,1], Laura L. Bourgeau-Chavez[a,2], Edwin A. Romanowicz[b,3], Suzy Brunzell[a,4], Curtis J. Richardson[b]

[a] Environmental Research Institute of Michigan, Ann Arbor, MI, USA
[b] Nicholas School of the Environment, Duke University, Durham, NC, USA

Received 11 March 2003; received in revised form 29 July 2003; accepted 18 August 2003

Abstract

A multi-year study was carried out to evaluate ERS synthetic aperture radar (SAR) imagery for monitoring surface hydrologic conditions in wetlands of southern Florida. Surface conditions (water level, aboveground biomass, soil moisture) were measured in 13 study sites (representing three major wetland types) over a 25-month period. ERS SAR imagery was collected over these sites on 22 different occasions and correlated with the surface observations. The results show wide variation in ERS backscatter in individual sites when they were flooded and non-flooded. The range (minimum vs. maximum) in SAR backscatter for the sites when they were flooded was between 2.3 and 8.9 dB, and between 5.0 and 9.0 dB when they were not flooded. Variations in backscatter in the non-flooded sites were consistent with theoretical scattering models for the most part. Backscatter was positively correlated to field measurements of soil moisture. The MIchigan MIcrowave Canopy Scattering (MIMICS) model predicts that backscatter should decrease sharply when a site becomes inundated, but the data show that this drop is only 1–2 dB. This decrease was observed in both non-wooded and wooded sites. The drop in backscatter as water depth increases predicted by MIMICS was observed in the non-wooded wetland sites, and a similar decrease was observed in wooded wetlands as well. Finally, the sensitivity of backscatter and attenuation to variations in aboveground biomass predicted by MIMICS was not observed in the data.

The results show that the inter- and intra-annual variations in ERS SAR image intensity in the study region are the result of changes in soil moisture and degree of inundation in the sites. The correlation between changes in SAR backscatter and water depth indicates the potential for using spaceborne SAR systems, such as the ERS for monitoring variations in flooding in south Florida wetlands.

Keywords: South Florida wetlands; ERS-2 SAR; Backscatter

1. Introduction

The ability of satellite imaging synthetic aperture radars (SARs) to detect forested wetlands was first demonstrated with L-band (24 cm wavelength) data from the Seasat satellite (Engheta & Elachi, 1982; Hess, Melack, & Simonett, 1990; Krohn, Milton, & Segal, 1983; Ormsby, Blanchard, & Blanchard, 1985). Since these initial studies, a number of researchers have shown that satellite SARs operating at both L-band and C-band (6-cm wavelength) can be used to map and monitor wetlands occupying a range of coastal and inland settings. These studies were carried out by using data from the Shuttle Imaging Radar (Alsdorf et al., 2000; Alsdorf, Smith, & Melack, 2001; Bourgeau-Chavez et al., 2001; Hess, Melack, Filoso, & Wang, 1995; Imhoff et al., 1987; Pope, Rejmankova, & Paris, 2001; Pope, Rejmankova, Paris, & Woodruff, 1997), ERS-1 and -2 (Brivio, Colombo, Maggi, & Tomasoni, 2002; Dwivedi, Rao, & Bhattacharya, 1999; Kasischke & Bourgeau-Chavez,

* Corresponding author. Current address: Department of Geography, University of Maryland, College Park, MD 20742, USA. Tel.: +1-301-405-2179.
E-mail address: ekasisch@geog.umd.edu (E.S. Kasischke).
[1] Currently at Western Regional Office, Ducks Unlimited, 3074 Gold Canal Drive, Rancho Cordova, CA 95670, USA.
[2] Currently with Ann Arbor Research and Development Center, Veridian Systems Division, P.O. Box 134008, Ann Arbor, MI 48113-4008, USA.
[3] Currently at Center for Earth and Environmental Sciences, State University of New York, Plattsburgh, NY, USA.
[4] Currently at Snohomish County, Public Works, 2731 Wetmore Avenue, Suite 300, Everett, WA 98201-3581, USA.

0034-4257/$ - see front matter © 2003 Elsevier Inc. All rights reserved.
doi:10.1016/j.rse.2003.08.016

1997; Moreau & Le Toan, 2003; Morrissey, Livingston, & Durden, 1994, Morrissey, Durden, Livingston, Stearn, & Guild, 1996; Ramsey, 1995; Ramsey, Nelson, Laine, Kirkman, & Topham, 1997; Rao et al., 1999; Townsend, 2001), JERS (Ormsby et al., 1985; Rosenqvist & Birkett, 2002; Rosenqvist, Forsberg, Pimentel, Rauste, & Richey, 2002; Townsend & Walsh, 1998), and Radarsat (Kandus et al., 2001; Parmuchi, Karszenbaum, & Kandus, 2002; Rio & Lozano-Garcia, 2000; Townsend, 2002; Werle, Martin, & Hasan, 2000; Zhou, Luo, Yang, Li, & Wang, 2000)]. In addition to mapping natural wetlands, researchers have demonstrated that spaceborne SARs can be used to monitor rice production (Kurosu, Masaharu, & Chiba, 1995; LeToan et al., 1997; Liew et al., 1998; Panigrahy et al., 1997; Ribbes & Le Toan, 1999; Rosenqvist, 1999; Shao et al., 2001), with the best results being obtained using C-band systems (ERS and Radarsat). In rice fields, growth of new in biomass in flooded rice fields result in significant increases (on the order of 6–8 dB) in C-band SAR image intensity (LeToan et al., 1997)).

A unique application for the current generation of imaging radar systems (ERS, JERS, Radarsat, and Envisat) is to monitor temporal variations in the hydrologic conditions present in wetlands. Tanis, Bourgeau-Chavez, and Dobson (1994) and Ramsey (1995) both used the same ERS data set to map the extent of coastal wetlands in Florida based on backscatter differences associated with flooded (during high tides) and non-flooded (during low tides) estuarine vegetation. Kasischke and Bourgeau-Chavez (1997) noted that distinct differences in radar backscatter occurred in different upland and wetland vegetation types in south Florida between ERS imagery collected during the wet and dry seasons of this semi-tropical region. Morrissey, Durden, Livingston, Stearn, and Guild (1996) showed that ERS SAR imagery could be used to discriminate between flooded and unflooded tundra on Alaska's North Slope, and that seasonal variations in temperature (freezing vs. thawing) strongly influenced radar backscatter. A number of studies showed that variations in flood stages along the Brazilian Amazon influenced the radar backscatter signatures from the SIR-C instruments (Hess et al., 1995; Alsdorf et al., 2000, 2001). Pope et al. (1997) noted changes in radar backscatter on SIR-C imagery based on flooded and non-flooded conditions in non-wooded wetlands in Central America. Finally, Townsend and colleagues (Townsend, 2001; Townsend & Foster, 2002; Townsend & Walsh, 1998) used time-series ERS, JERS, and Radarsat imagery to monitor seasonal patterns of flooding in wooded wetlands located along rivers.

In this paper, we present the results of a multi-year study designed to assess the potential for using C-band ERS synthetic aperture radar (SAR) imagery to monitor wetland hydrology in south Florida. This study was initiated during the spring of 1997 to more fully investigate the sources of backscatter variations observed in the ERS SAR images collected over south-central Florida wetlands. The overall goal of this study was to correlate the seasonal responses in ERS radar backscatter signatures associated with changes in hydrologic status and vegetation cover in order to develop approaches to use spaceborne SAR data to monitor regional-scale hydropatterns in the wetland ecosystems of this region.

2. Previous satellite SAR studies of south Florida Wetlands

The results presented in this paper extend those from previous studies of satellite SAR imagery in this region (Bourgeau-Chavez et al. 1996; Kasischke & Bourgeau-Chavez, 1997; Kasischke, Bourgeau-Chavez, Smith, Romanowicz, & Richardson, 1997). Kasischke and Bourgeau-Chavez (1997) initially assessed the utility of ERS SAR imagery to monitor variations in radar backscatter associated with changes in soil moisture and surface inundation during the wet and dry seasons in southwestern Florida. Relative radar backscatter measurements from 10 different vegetation types were compared from ERS SAR imagery collected during the dry (April) and late wet (October) seasons of 1994. Field observations of water level/soil moisture were made during October and either directly observed or inferred for April based on precipitation patterns. The results showed that the radar backscatter either increased between April and October due to an increase in soil moisture, or decreased where the ground surface transitioned from a wet soil to a flooded condition.

During 1995, a more intensive study was carried out using nine ERS SAR scenes collected between May and November, which spans the typical wet season in this region. Water levels were measured along several transects in 10 study sites with different vegetation covers in the same areas studied (Kasischke & Bourgeau-Chavez, 1997). In the sites dominated by woody vegetation, the changes in water levels did not result in changes in backscatter because: (a) the sites were continuously flooded, and therefore changes in water levels did not result in changes in scattering; or (b) the overstory canopy was dense enough that the total backscatter signature changes from flooding were attenuated by the canopy itself. In sites dominated by non-woody vegetation, there was an overall decrease in ERS backscatter as water level increased, with the level of decrease being related to live vegetation density (Bourgeau-Chavez et al., 1996).

Additional ERS SAR data were collected at roughly monthly intervals over south-central Florida in 1995 and 1996. The geographic focus was shifted slightly to the east to encompass sites within the boundaries of the Big Cypress National Preserve as well as the Everglades National Park (Fig. 1). These regions contained sites that were quite similar to those studied by Bourgeau-Chavez et al. (1996) and Kasischke and Bourgeau-Chavez (1997), but included additional vegetation cover types characteristic of this region. Kasischke et al. (1997) showed that not only did dramatic variations occur throughout all non-woody wetlands throughout the wet season/dry season cycle, but that

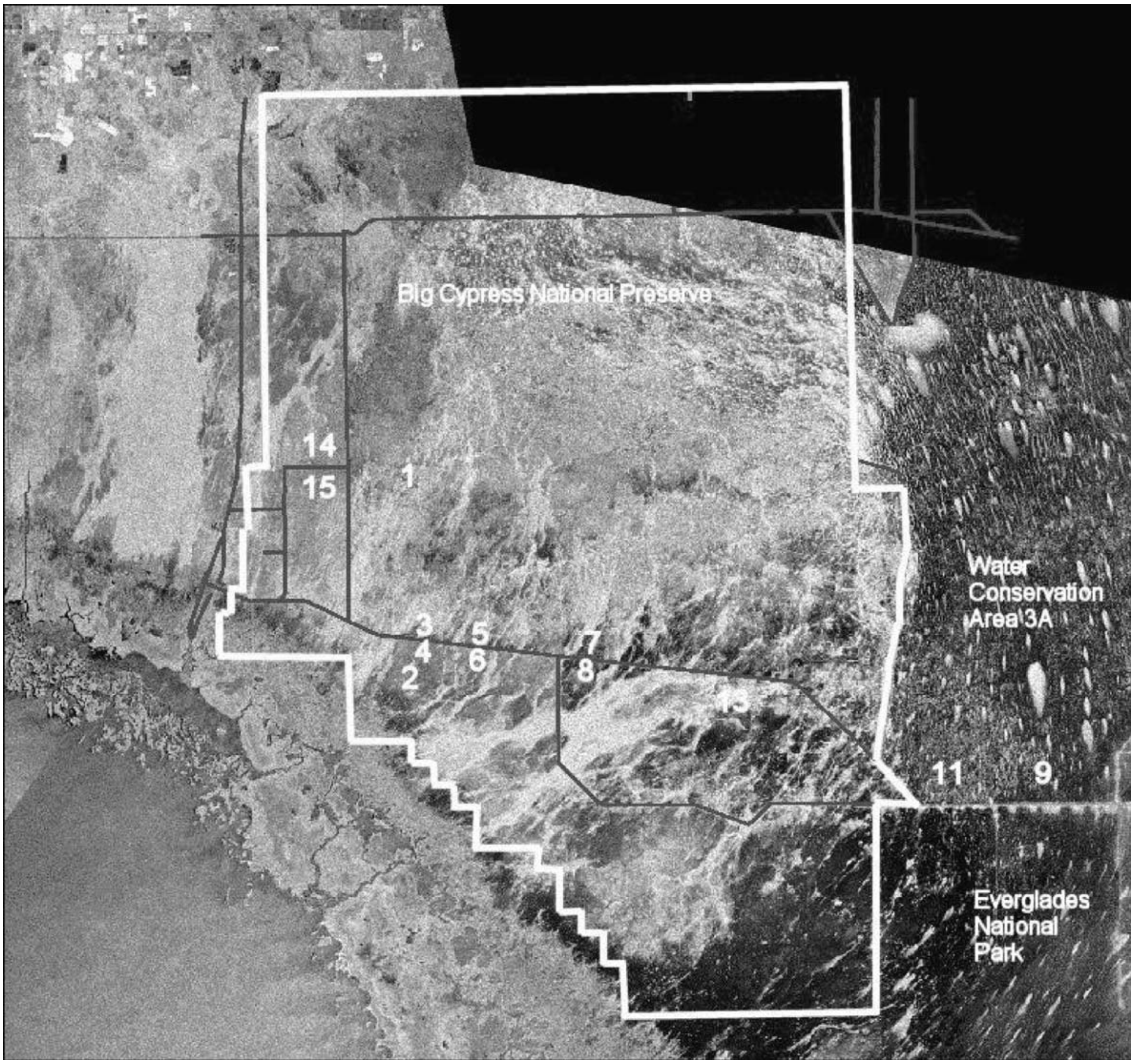

Fig. 1. ERS SAR image mosaic of the south-central Florida region containing the region investigated in this study and previous research. The white polygon in the center is the boundary of the Big Cypress National Preserve, while each number represents the location of a site used in the present study.

significant differences in radar backscatter occurred between years because of variations in seasonal precipitation patterns. In addition, this study showed that decreases in radar backscatter also occurred during the dry season in some sites, most likely due to decreases in soil moisture.

The results from these studies clearly showed that seasonal variations in level of water inundation in wetlands during the wet season, as well as variations in soil moisture in non-flooded sites during the dry season both have strong influences on ERS SAR image intensity. As discussed by Kasischke and Bourgeau-Chavez (1997), additional variations in radar backscatter in these ecosystems resulted from differences in the levels of tree cover as well as levels of aboveground biomass in these ecosystems.

One additional study that relates to the one presented in this paper is that conducted by Pope et al. (1997), who used C- and L-band radar imagery from SIR-C to examine variations in radar backscatter over 11 marshes in Central America dominated by non-woody (macrophyte) vegetation. These sites were imaged during the dry and wet seasons, with 10 of the sites experiencing measurable increases in water depth during the wet season. In three sites dominated by dense (>60% vegetation cover) and large-stemmed marsh vegetation (cattail and saw grass), there was an increase in radar backscatter associated with flooding. In the seven sites dominated by lower density (<50%), large-stemmed marsh vegetation or small-stemmed vegetation (rushes) of variable density (50 to 80%), there was a decrease in radar backscatter associated with flooding.

3. Expected influence of seasonal wetland hydrologic variations on ERS SAR backscatter measurements

The seasonally variable hydrologic conditions occurring in south Florida's wetlands should result in a predictable trajectory of change in the radar backscatter measurements obtained from the ERS SAR. Sites exposed to inundation or flooding during the wet season and no flooding during the dry season should experience three distinct hydrologic regimes: (a) a period of increasing soil moisture during times of increasing precipitation at the beginning of the wet season; (b) a period where water covers or inundates the ground surface to various depths during the middle of the wet season; and (c) a period of decreasing soil moisture in the middle of the dry season when precipitation levels decrease sharply.

In terms of radar backscatter or the measured backscatter coefficient, σ^o, two wetland types within the study site need to be considered: those containing only herbaceous vegetation and those containing shrubs and trees in addition to the herbaceous vegetation. The total backscatter from wetlands dominated by herbaceous vegetation ($\sigma^o_{\text{t-h}}$) can be modeled after Kasischke and Bourgeau-Chavez (1997) as

$$\sigma^o_{\text{t-h}} = \sigma^o_c + \tau^2_c(\sigma^o_s + \sigma^o_m) \tag{1}$$

where σ^o_c is the backscatter coefficient from the vegetation canopy, τ_c is the transmission coefficient of the vegetation canopy, σ^o_s is the backscatter from the ground surface, and σ^o_m is the backscatter from multiple-path scattering between the surface and the vegetation canopy. For wetlands containing woody vegetation, the backscattering coefficient ($\sigma^o_{\text{t-w}}$) is modeled as

$$\sigma^o_{\text{t-w}} = \sigma^o_c + \tau^2_c\tau^2_t(\sigma^o_s + \sigma^o_t + \sigma^o_d + \sigma^o_m) \tag{2}$$

where, in this case, σ^o_c is the scattering from the crown layer of smaller woody branches and foliage as well as the herbaceous vegetation, σ^o_t is the direct scattering from the tree trunks, τ_t is the attenuation of microwave energy by the tree trunks, σ^o_d is a double-bounce scattering between the trunks and the ground, and σ^o_m accounts for multiple-path scattering between the ground and canopy.

In our study, we used the MIchigan MIcrowave Canopy Scattering (MIMICS) model (Ulaby, Sarabandi, McDonald, & Dobson, 1990) to examine the influence of site conditions (water depth, soil moisture, and canopy cover) on the expected ERS SAR backscatter measurements from wetlands with herbaceous cover (Eq. (1)) following the approach of Dobson, Ulaby, and Pierce (1995). The MIMICS model was exercised using soil moisture and biomass levels that covered the range of site conditions encountered in this study. The vegetation in the herbaceous wetlands was assumed to consist primarily of sedges, grasses, and reeds (rushes), and modeled as vertical dielectric cylinders that were uniformly distributed.

The MIMICS model was exercised using soil moisture levels ranging from 0 to 1 cm^3 cm^{-3} and biomass levels ranging from 0.0 to 1.68 kg m^{-2}. We selected the biomass levels using data from one of our study sites as a baseline (Site 4 with average biomass of 0.42 kg m^{-2}, density of 250 stems m^{-2} and height of 55 cm). We assumed that the canopy height and weight per stem were constant and created new biomass levels by varying the stem density between 0 and 1000 stems m^{-2} for the different model runs. For all cases except the no biomass case, we also exercised MIMICS assuming a flooded ground surface (e.g., standing water of 5 cm depth). For all model runs, we assumed system and imaging parameters corresponding to the ERS SAR, e.g., a 5.6-cm wavelength, VV polarization and incidence angle of 23°.

Fig. 2 presents the MIMICS results consisting of the backscatter coefficient as a function of soil moisture and aboveground biomass. These results figure illustrate three

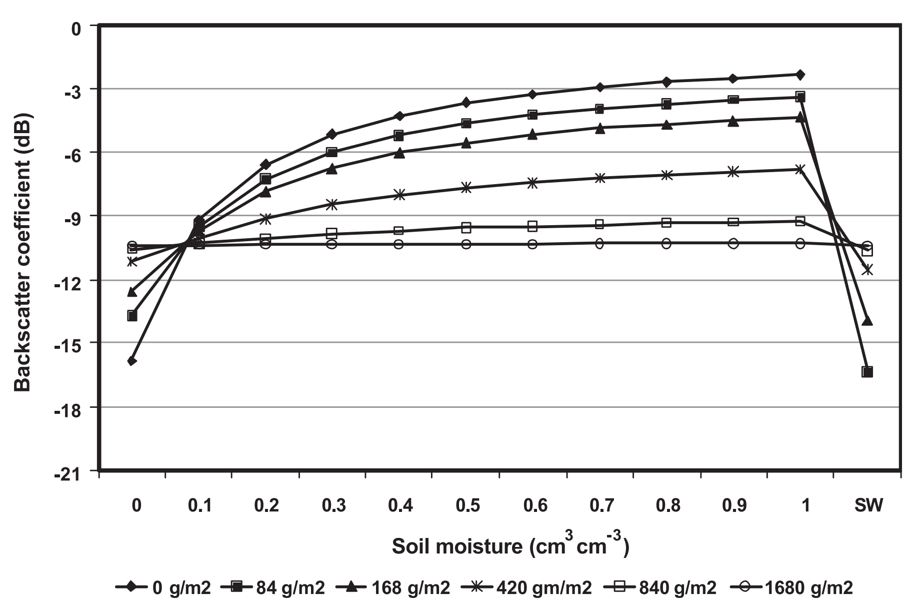

Fig. 2. Variations in ERS backscatter as a function of aboveground biomass and soil moisture for marl prairie wetland vegetation based on predictions from the MIMICS theoretical microwave scattering model.

different processes: (a) the response of microwave backscatter to increases in soil moisture; (b) the response of microwave backscatter to changes from a non-flooded to flooded state; and (c) the response of microwave backscatter to increases in aboveground, live biomass. In all biomass level cases, we see an increase in backscatter as soil moisture increases. In addition, we see a sharp decrease in backscatter when the site goes from a flooded to a non-flooded state.

The complex role of vegetation is illustrated in Fig. 2. When soil is perfectly dry (soil moisture=0), there is little or no forward and very little backward scattering of incident microwave energy. In the no soil moisture case (0 cm^3 cm^{-3}), as biomass increases, there is an increase in direct canopy scattering (σ_c^o), but there is little or no contribution from the multiple-interaction scattering (σ_m^o). This situation changes when the surface is flooded. In this case, there is no backscattering of energy from the ground surface, and the backscattered energy comes entirely from the vegetation through direct canopy or multi-path scattering. The fact that, in all biomass cases, the backscatter in the flooded cases is lower than that in the dry soil cases indicates that MIMICS predicts there is no multi-path scattering occurring in the flooded scenario. The decrease in backscatter as a function of biomass at all soil moisture levels is the result of vegetation's role as an attenuator (τ_c) of direct scattering from the soil surface.

The results from Fig. 2 are representative of the biomass levels observed at most of our non-woody study sites. The results from Pope et al. (1997) indicate that at some point the size and structure of stems play a role in determining the degree of multiple-path scattering that occurs in non-woody wetlands. The study of Pope et al. (1997) contained vegetation types (cattail and sawgrass) with much larger stem sizes than the vegetation found in the sites used in the present study. In sites with high vegetation cover and large-stem sizes, Pope et al. (1997) observed increases in backscatter when sites became flooded, which is identical to the response that has been observed in wetlands with dense, woody vegetation.

Based on the MIMICS outputs in Fig. 2 and observations from other studies, we developed a prediction of how we expect variations in seasonal flooding and soil moisture to influence the ERS backscatter signature in the non-wooded study wetlands in the south Florida. In this prediction, we assumed that: (a) soil moisture first decreases from 1.0 to 0.10 cm^3 cm^{-3} during the beginning of the dry season and then increases from 0.10 to 1.0 cm^3 cm^{-3} as the dry season transitions to the wet season; (b) the site has an average biomass level of 400 g m^{-2}; (c) the average vegetation height is 50 cm; and (d) the water depth during the wet season reaches 25 cm. Fig. 3 shows the expected changes in backscatter for these conditions. Note that as water level at the site increases, there is a decrease in backscatter because the water reduces the amount of vegetation available for direct backscatter to radar. The results in Fig. 3 represent the overall trends we expect to observe in the multi-date ERS SAR imagery collected over south Florida, and may in fact not exactly match the exact magnitude of change in the actual data.

The expected changes in the wooded wetland sites are a little more difficult to predict. In previous studies, radar backscatter in wooded wetlands has been shown to increase when they become flooded because of increases from the multiple-scattering terms in Eq. (2) (σ_d^o, σ_m^o). However, the tree density in our sites is quite low, so we expected the increase in backscatter to be lower than observed in riparian wetlands, which contain dense forest

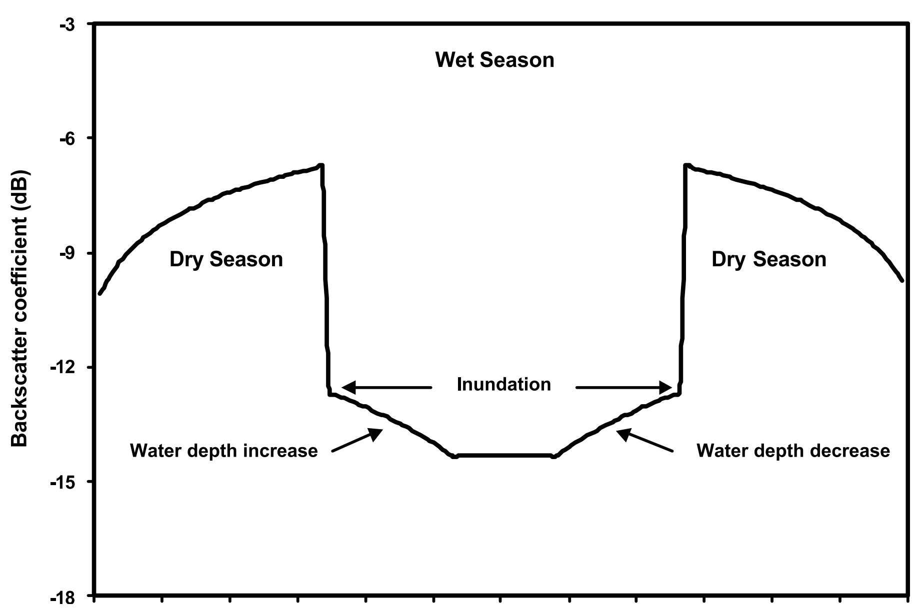

Fig. 3. Expected seasonal variations in ERS radar backscatter for marl prairies under different hydrologic patterns in the south Florida region.

canopies. Because of the low tree density, and overall low biomass of the underlying herbaceous vegetation in the wooded sites, we would expect these sites to exhibit variations associated with variable soil moisture as well.

4. Methods

Field studies were designed to address five hypotheses on the relationship between radar backscatter and scene conditions depicted in Fig. 3:

Hypothesis 1. During the dry season, in sites that do not have standing water, radar backscatter on ERS SAR imagery will vary in proportion to soil moisture.

Hypothesis 2. As non-wooded wetland sites become inundated with standing water as the wet season between May and October progresses, radar backscatter on ERS SAR imagery will decrease. Wooded wetlands may experience a decrease or increase in backscatter depending upon the density of the trees present.

Hypothesis 3. As water depth increases in non-wooded wetlands, backscatter will decrease.

Hypothesis 4. In flooded sites, ERS radar backscatter should increase as biomass increases.

Hypothesis 5. The sensitivity of ERS radar backscatter measurements to variations in water level and soil moisture will decrease as the levels of aboveground live biomass increases.

To test these hypotheses, we instrumented test sites in southern Florida with automatic water depth gauges, and collected additional observations designed to quantify varia-

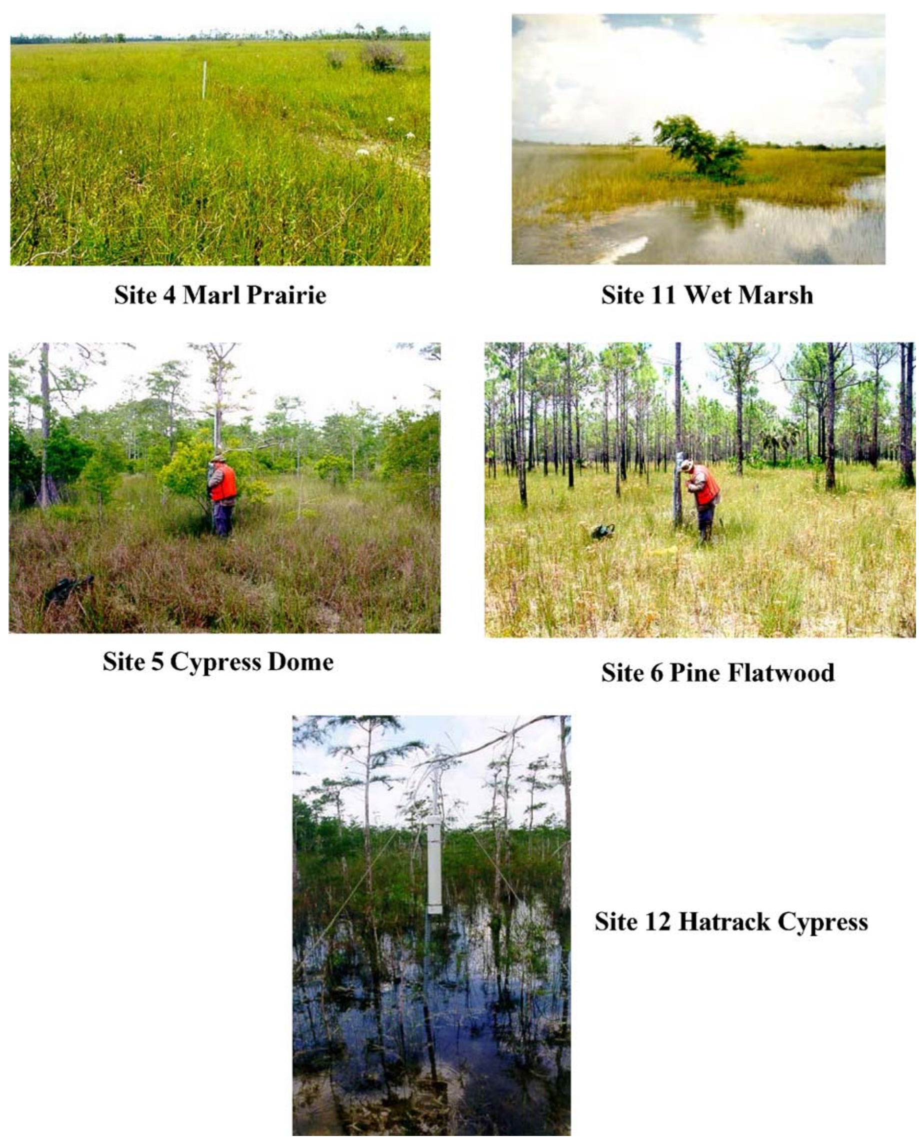

Fig. 4. Ground photographs of the different wetland types from sites used in this study.

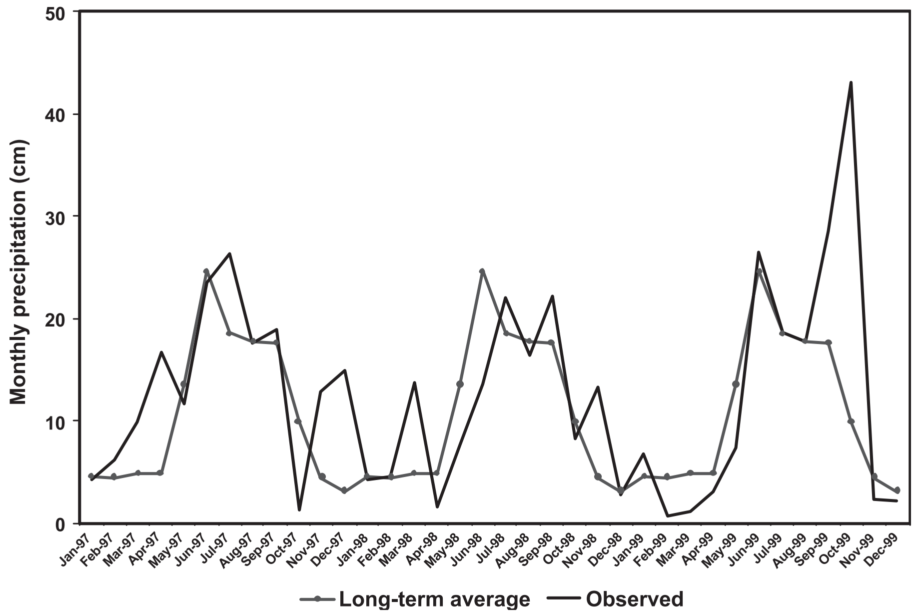

Fig. 5. Monthly precipitation totals based on data collected at three precipitation gauges operated for this study and data reported from the Tamiami Trail 40 Mile Bend station.

tions in vegetation cover, soil moisture, and topography at each site. Over a 25-month period between June of 1997 and August of 1999, the instrumented test sites were imaged on 22 different occasions by the C-band (5.6-cm wavelength), VV polarized SAR system onboard the ERS-2 platform. Radar backscatter measurements were extracted from the ERS SAR imagery for each study site and correlated with the field data.

4.1. Study area characteristics

Several different wetland types found within the Big Cypress National Preserve (BCNP) and the Everglades located in south-central Florida were the focus of this study. The BCNP is an extended system of wetlands interspersed with drier upland sites, and covers an area of 295,000 ha. The distribution of wetlands in the study region is controlled by a combination of physiographic and climatic variables. The topography of the region is characterized by gently sloping terrain from mean sea level (MSL) in the south to 6 m above sea level in the northeastern portion of the Preserve (average slope=0.005 m km^{-1}); however, small variations in topography have a strong control on site drainage characteristics. The underlying geology of the region consists of the Tamiami Formation, limestone that was formed during the Miocene. The soils are mostly entisols, with layers of very poorly drained marl or peat soils to well-drained sandy soils all overlying limestone (Brown, Stone, & Carlilse, 1990).

The climate of the region has been described as subtropical or tropical savanna, with nearly 80% of the annual precipitation (130 cm) occurring in the wet season (May to

Table 1
Summary of intensive study sites

Site	Vegetation type	Water monitoring period
1	Marl prairie	6-20-97 to 8-23-99
2	Marl prairie	2-15-98 to 8-23-99
3	Marl prairie	6-21-97 to 7-31-99
4	Marl prairie	6-27-97 to 7-26-99
5	Cypress dome	6-21-97 to 7-31-99
6	Pine flatwood	6-21-97 to 8-2-99
7	Marl prairie	6-21-97 to 8-25-99
8	Marl prairie	6-21-97 to 8-5-99
9	Wet marsh	
11	Wet marsh	
12	Hatrack cypress	7-7-98 to 8-23-99
14	Marl prairie	7-9-98 to 8-27-99
15	Marl prairie	7-9-98 to 8-27-99

Table 2
Summary of observed precipitation

	Long-term Average	1997	1998	1999
Total precipitation (cm)	128.0	162.2	129.9	160.6
Percent of long-term average		126.7	101.5	125.4
	Long-term Average	1997	1998	1999
Wet season precipitation (cm)	101.9	99.2	89.9	141.4
Percent of long-term average		97.3	88.2	138.8
	Long-term Average	1997/1998	1998/1999	
Dry season precipitation (cm)	26.1	51.7	30.7	
Percent of long-term average		197.7	117.5	

October) and near drought conditions in the dry season (November to April) (Duever et al., 1986; Duever, Meeder, Meeder, & McCollom, 1994). There is also a great deal of long-term variability in precipitation patterns, resulting in decadal-scale periods of drier and wetter conditions. The annual precipitation patterns result in seasonal flooding and drying of many of the wetlands in this region. In most years, water levels reach maximum levels by fall (September and October), and minimum levels during the spring (March and April) (Gunderson, 1994).

Minor variations in topographic relief and soil drainage result in a complex spatial distribution of different vegetation and wetland types. Initial classification of ecosystems in this region is based upon the hydro-edaphic conditions of a site, with wetlands having soils that are saturated part of the year and uplands having soils that are not (Gunderson, 1994). Pine flatwoods and hardwood hammocks can be found in upland areas of higher relief. In poorly drained areas where the bedrock is shallow, marl prairies, wet marshes, and hatrack cypress dominate. Finally, cypress domes and tropical hardwood swamps are the cover types found in the most poorly drained sites near sloughs or areas with accumulated peat.

4.2. Study sites and field observations

Since previous studies showed that forested swamps with dense canopy covers were not amenable to monitoring using the ERS SAR (Bourgeau-Chavez et al., 1996; Kasischke et al., 1997), we focused our efforts on two categories of wetlands: (a) wet marshes and marl prairies dominated by herbaceous vegetation; and (b) wetlands with

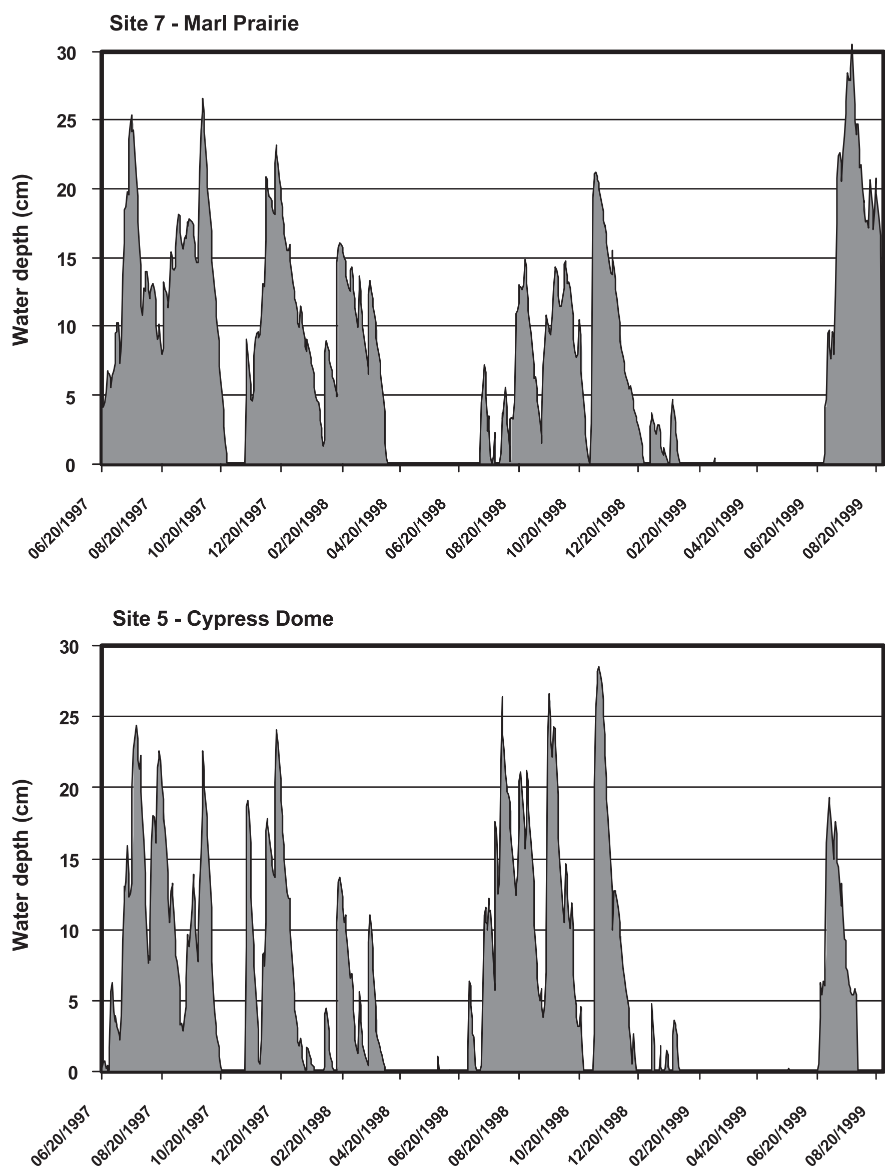

Fig. 6. Measured water depths at two study sites.

Table 3
Average biomass and canopy height in marl prairie sites

Site	1	2	3	4	7	8	14	15
Average biomass (kg m^{-2})	0.20	0.27	0.87	0.42	0.33	0.29	0.36	0.22
Height (cm)	51	33	83	55	44	61	65	55

sparse, open tree and shrub canopies including hatrack cypress, cypress domes, and pine flatwoods (Fig. 4). Fifteen potential test sites within the BCNP and western Everglades region were identified during an initial field trip in early 1997 (Fig. 1). The positions of each site were determined using a global positioning system (GPS), as were the locations of easily identifiable features (such as road intersections) to allow for geometric registration of the ERS SAR imagery. Subsequently, only 13 of these sites were instrumented (Table 1) because it was decided to reserve instruments as backups in case of equipment breakdowns that were likely to occur over the course of the study. Eight (8) of these sites were located in marl prairies, two (2) in wet marshes, and three (3) in sparsely wooded pine or cypress stands (Fig. 1 and Table 1).

Nine sites were established in June of 1997 (see Table 1), and equipped with a water monitoring station (a pressure transducer linked to a data logger that recorded water level every 30 min). The surface topography for each 200-m^2 site was surveyed to determine if any small-scale topographic variations were present. No such variations were found in any of the sites, which were essentially flat. Site 3 was instrumented in February 1998, while Sites 12, 14, and 15 were instrumented in August 1998. To complement climate data from existing weather stations, three rain gauges were

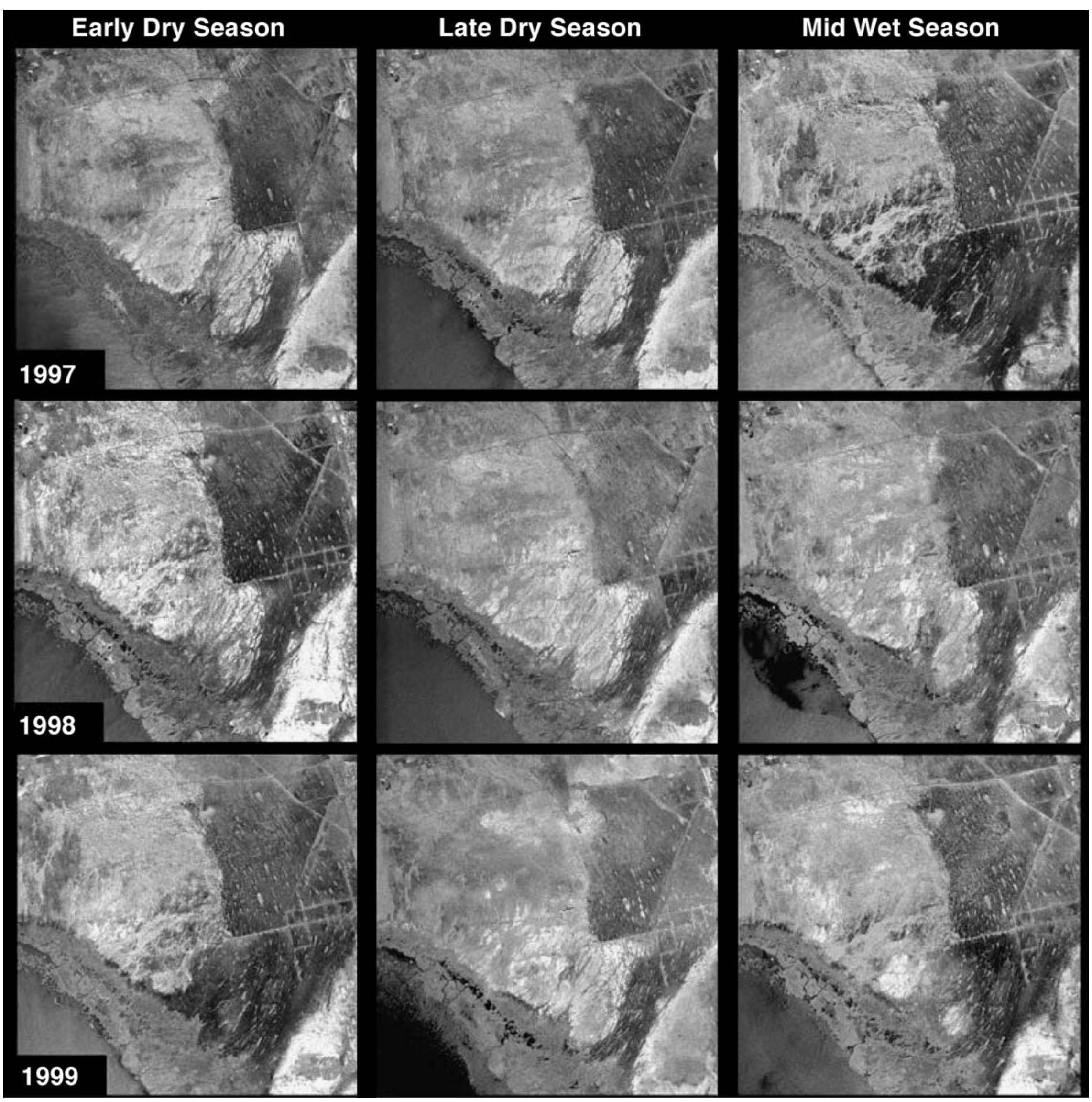

Fig. 7. ERS SAR images of the study region from 1997 to 1999.

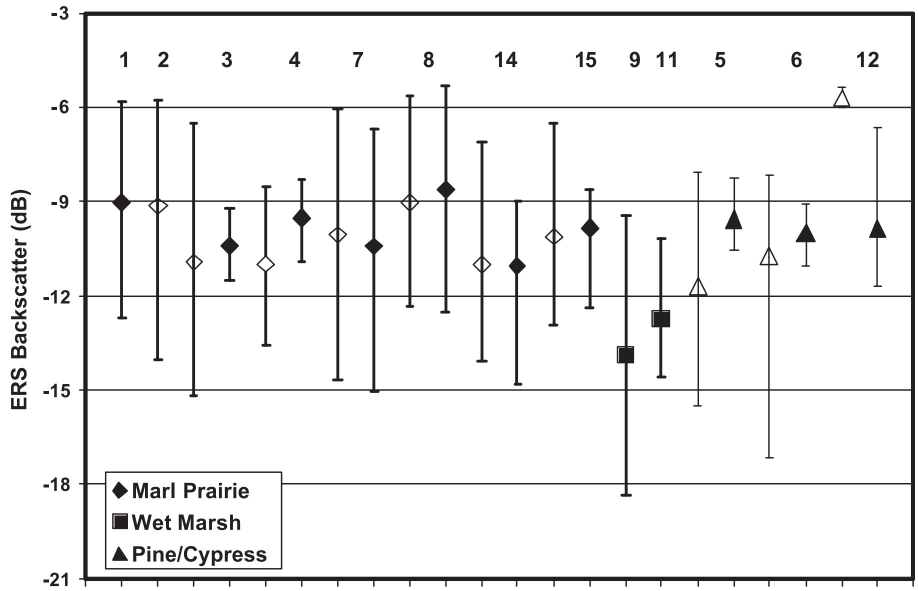

Fig. 8. ERS radar backscatter measurements from 13 different test sites over the entire study period. The unfilled symbols represent the average backscatter measurements from the unflooded observations, while the solid symbols represent the average backscatter measurements from flooded observations. The error bars present the minimum and maximum backscatter measurements for each site.

also installed, and subsequently operated between October 1997 and July 1999.

Field measures of soil type, soil moisture, and vegetation characteristics (type, biomass, density, height, etc.) were collected during nine field campaigns spaced at approximately 3-month intervals throughout the course of the project. Soil moisture samples were collected coincident with the satellite overpasses at sites that were road-accessible and non-flooded at selected times throughout the study. During each collection, soil samples were collected with an 11-cm-diameter soil corer to a depth of 10 cm at five points randomly located in each study site. The samples were immediately placed in a plastic bag, transported to a lab, weighed and then dried for 72 h at an oven temperature of 65 °C, and reweighed. Volumetric soil water (W_v) (in cm^3 of water per cm^3 of soil or cm^3 cm^{-3}) was computed as:

$$W_v = D_b W_g \tag{3}$$

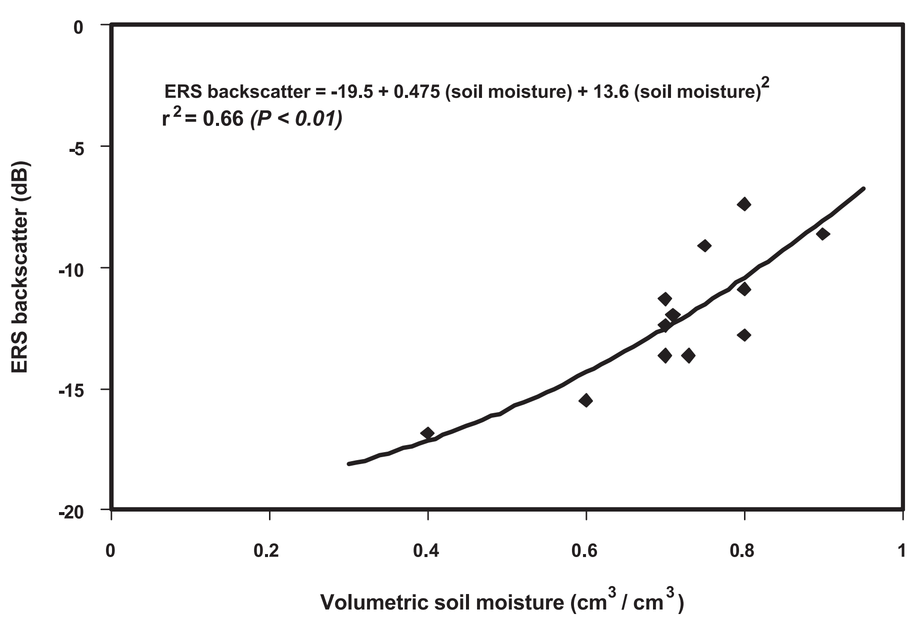

Fig. 9. ERS radar backscatter as a function of soil moisture in unflooded marl prairie sites.

where D_b is the bulk density of the soil and W_g is the gravimetric moisture content of the soil. Bulk density of the soil was calculated as

$$D_b = W_d / V \quad (4)$$

where D_w and V are the dry weight (g) and volume (cm^3) of the soil sample, respectively. Gravimetric moisture was calculated as

$$W_g = (W_w - W_d)/W_d \quad (5)$$

where W_w is the wet weight of the soil sample.

Soil moisture and coincident radar imagery were collected on two dates in 1998 and three dates in 1998. At many of the sites, the soils were either flooded or saturated with water, and no samples were collected. From the five data collections, 12 pairs of soil moisture/backscatter data were available for analysis.

Vegetation samples were collected at the six marl prairie sites during each field campaign. Five 0.25×0.25 quadrats were randomly located in each site, and all aboveground vegetation harvested and bagged. The heights of 5 stems were measured in each sample. Each sample was weighed and then dried for 72 h at an oven temperature of 65 °C and reweighed.

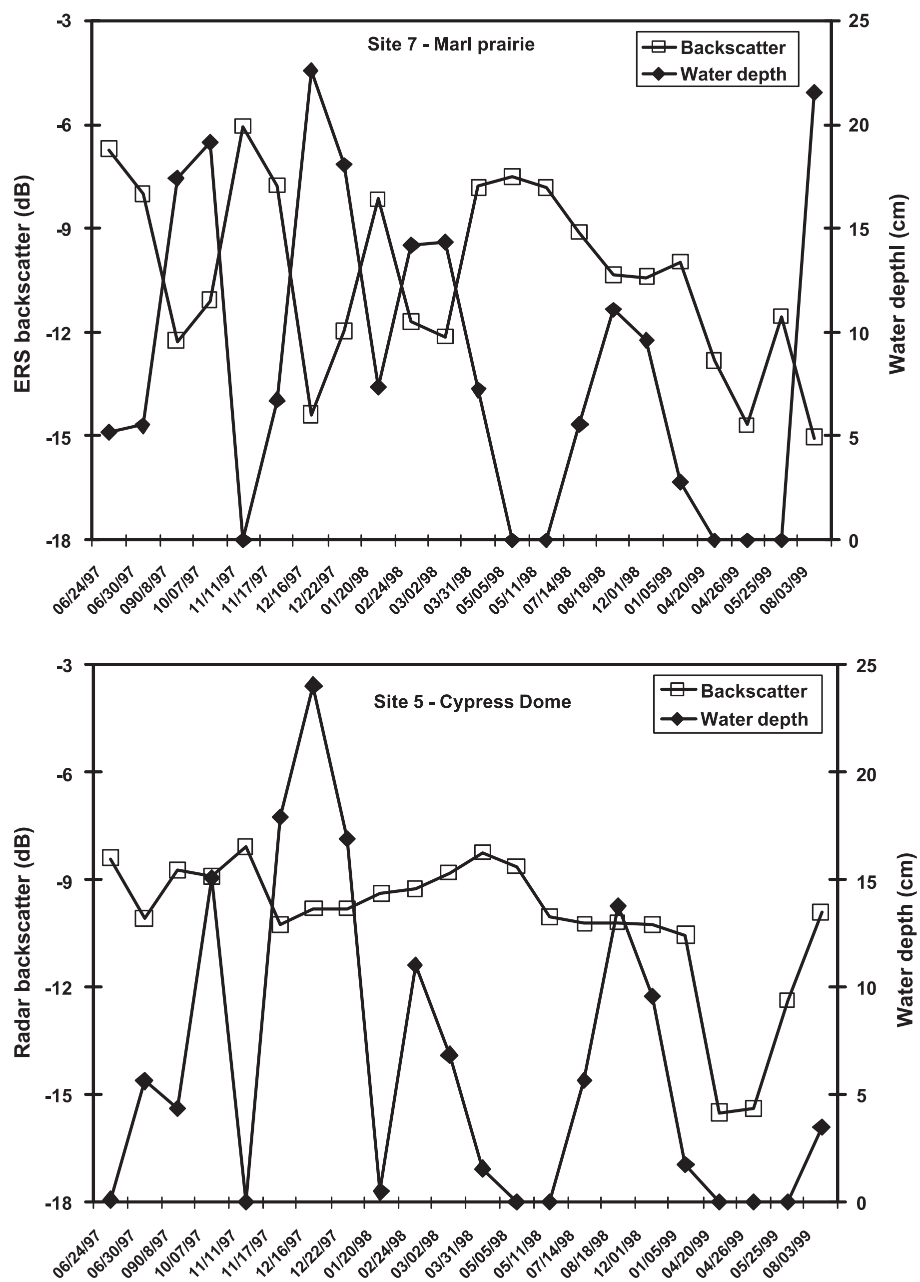

Fig. 10. ERS radar backscatter and water level measurements made at Site 7 and Site 5 between June 1997 and August 1999.

The dried sample weights were then used to estimate aboveground biomass.

Finally, the study was designed to begin to investigate the influence of water control structures (in the form of raised road beds and adjacent drainage ditches or canals) on wetland hydrology. Four pairs of sites in similar vegetation cover types were used, with one site located up gradient from a water control feature, and the other down gradient. These paired sites included: Sites 3 and 4; Sites 5 and 6; Sites 7 and 8; and Sites 14 and 15 (Fig. 1). In all cases, the water control feature consisted of a raised roadbed that impeded the natural north to south flow of water. At three of the paired sites, the roadbed was approximately 3 m above the surrounding wetlands with an adjacent drainage canal (2–3 m deep) on the north side and large, cement drainage structures (located periodically at a spacing of 500–1000 m) running underneath the road. At one paired site (Sites 14/15), the roadbed was only 25 cm above the wetlands, and with small (30–40 cm diameter) metal drainpipes placed under the road.

4.3. ERS SAR imagery

SAR imagery from the ERS-2 satellite for this study was provided through a data grant from the European Space Agency (Experiment AO2.USA133). ERS SAR images were collected on 22 different dates between 24 June 1997 and 3 August 1999. The ERS imagery was collected with a frequency that averaged once every 36 days, although the shortest time period between images was 6 days and the longest was 75 days. Ten (10) of these images were collected during what is considered to be the wet or rainy season (May to October), while twelve (12) were collected during the dry season (November to April).

To radiometrically correct the ERS SAR imagery, we used sensor calibration coefficients provided by the European Space Agency and image processing software created by ERIM International. Studies have shown the ERS-2 SAR instrument to be radiometrically stable, allowing for within scene (relative) calibration to within ± 0.5 dB and between scene (absolute) calibration to within ± 1.5 dB (Meadows, Laur, & Shattler, 1999). The different images were georeferenced using ERDAS-IMAGINE software. Mean backscatter values were determined by averaging 16×16 pixels (a 200×200 m^2 area) surrounding each study site. This number of samples results in a 90% confidence interval of ± 0.7 dB (Ulaby, Moore, & Fung, 1982).

5. Results

5.1. Hydrologic conditions

Fig. 5 and Table 2 summarize the precipitation patterns during the study period. The long-term average rainfall for the region is based on precipitation records collected at the Tamiami Trail 40 Mile Bend station (25°46′ N lat., 80°49′ W long.). The observed precipitation is based on the average of the observations collected for this study and the data collected at the Tamiami Trail station.

The total annual precipitation during 1998 was near normal, while precipitation levels for 1997 and 1999 were above the long-term average by 25% (Table 2). However, the rainy season (May–October) in 1997 had near normal levels of precipitation, in 1998 slightly below normal, and in 1999 significantly above normal. Finally, during the dry season between November 1997 and April 1998, the precipitation was almost twice the long-term average, while for the same period in 1998/1999, it was slightly only above normal.

Fig. 6 presents examples of the measured water depths for two sites, and shows the variations in water depth are related to seasonal precipitation patterns. Each site experienced variable water depth levels during the wet season, and non-flooded conditions during the dry season. However, the patterns of flooding and non-flooding were different between sites and between years. The data loggers at the wet marsh

Table 4
Summary of variations in average ERS radar backscatter (dB) for flooded and non-flooded conditions in the south Florida study sites

Sites	Flooded 1997/1998	Flooded 1998/1999	Unflooded 1998	Unflooded 1999	Unflooded 1998 vs. unflooded 1999	Unflooded 1998 vs. flooded 1997/1998	Unflooded 1999 vs. flooded 1998/1999
Marl prairie sites							
2			−7.0	−13.3	−6.3		
3	−10.4	−11.1	−10.1	−14.5	−4.4	−0.3	3.4
4	−9.5	−9.5	−8.7	−13.0	−4.3	−0.8	3.5
7	−10.1	−10.5	−7.7	−13.0	−5.3	−2.4	2.5
8	−8.3	−8.5	−6.6	−11.8	−5.2	−1.7	3.3
14	−9.0	−11.0	−7.3	−13.1	−5.8	−1.7	2.1
15	−8.8	−10.8	−6.7	−12.4	−5.7	−2.2	1.6
Average	−9.4	−10.2	−7.7	−13.0	−5.3	−1.5	2.7
Cypress/pine sites							
5	−9.3	−9.7	−8.9	−14.4	−5.5	−0.4	4.8
6	−9.9	−9.9	−9.0	−15.2	−6.1	−0.9	5.3
12	−9.1		−5.7			−3.4	
Average	−9.5	−9.8	−7.9	−14.8	−5.8	−1.6	5.0

sites (Sites 9 and 11) experienced numerous failures due to insect infestations and higher than expected water levels. Because of this, limited data from these sites were available. At no time were the water depths at these sites less than 30 cm when the sites were visited, and during several visits, they were >80 cm in depth. These two sites experienced the deepest levels of inundation of all sites. The maximum levels of inundation at the other sites were between 25 and 30 cm. Site 2 experienced very little flooding at all.

The water level data showed that the individual study sites experienced different hydroperiods, e.g., the length of time during which a wetland is flooded or inundated. For sites where water-level data were available throughout the study period (Sites 1, 3–8), the average water depth during the 1997 wet season was higher than the 1998 wet season (average of 8.0 vs. 7.2 cm). Similarly, the average water depth during the 1997/1998 dry season was higher than during the 1998/1999 dry season (average of 4.7 vs. 2.8 cm). These observations are consistent with the precipitation patterns in Table 2. In two pairs of sites where water control structures existed, the up-gradient site was drier than the down-gradient site (Sites 3/4 and 14/15), while in the two other pairs of sites, the up-gradient site was wetter than the down-gradient site (Sites 5/6 and 7/8).

Finally, overall, the soils found within the marl prairie sites were very poorly drained, and these soils were frequently saturated even when the sites were not flooded. The lowest soil moisture measured in these sites was 0.41 $cm^3\ cm^{-3}$ in April of 1999 after a period of low precipitation.

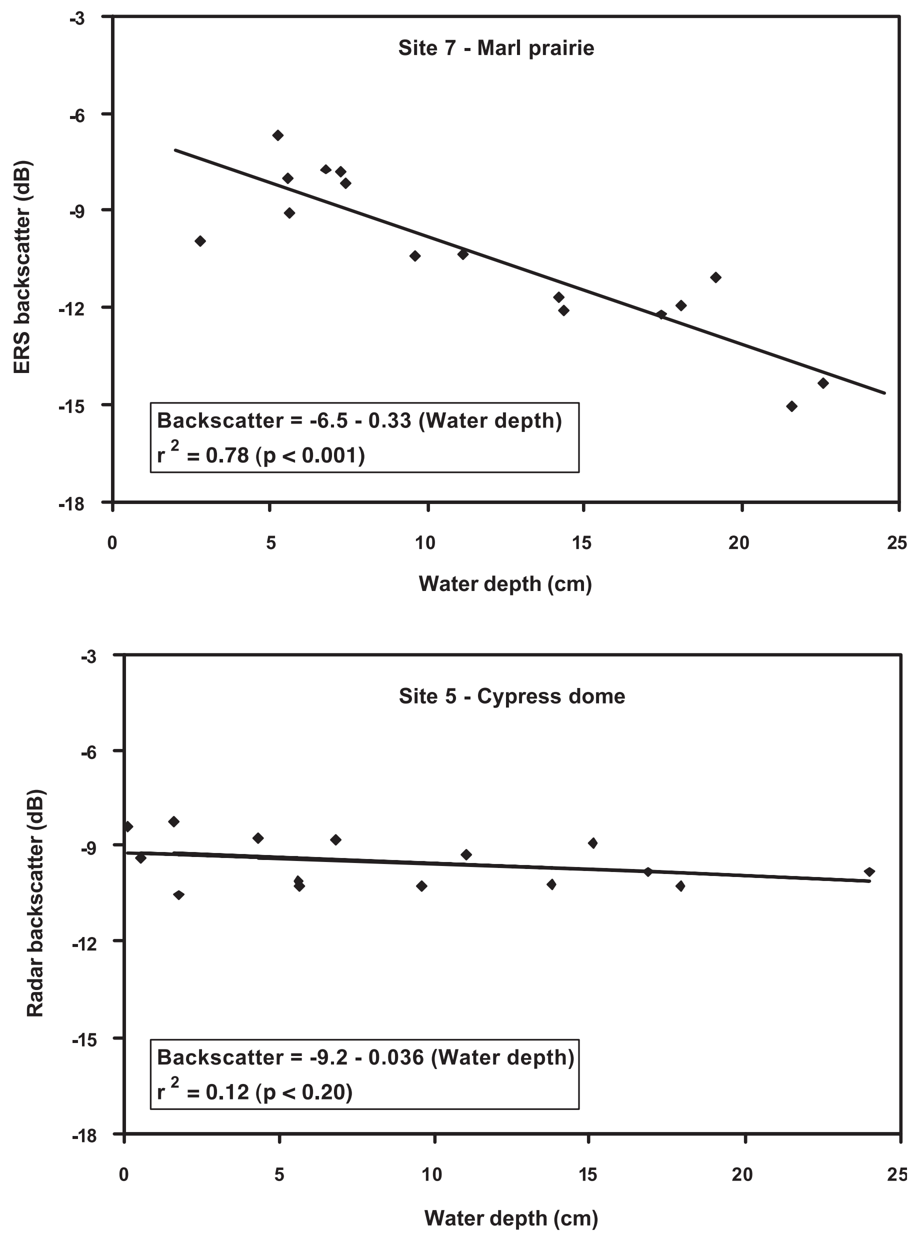

Fig. 11. Variation in ERS radar backscatter as a function of water depth from data collected at Site 7 and Site 5.

5.2. Vegetation measurements

Table 3 summarizes the average aboveground biomass levels and heights measured for the different sites. No seasonal trends were detected in the average biomass and height levels at any site.

5.3. Comparison of radar backscatter with soil moisture, water level, and biomass measurements

Fig. 7 presents examples of the ERS SAR imagery collected over the study region during the early dry, late dry and middle wet seasons of 1997 to 1999. The range in variation in image intensity during the study period matches those observed during previous studies in this area by Bourgeau-Chavez et al. (1996) and Kasischke et al. (1997).

Fig. 8 presents a summary of the average ERS radar backscatter measurements obtained for the different sites over the entire course of the study. The lowest average backscatter measurements were observed in the wet marsh sites (−13.2 dB) that experienced nearly continuous flooding. There was little difference in the average backscatter of the marl prairie sites (−9.9 dB) and the cypress/pine sites (−10.1 dB). In both the marl prairie and cypress/pine sites, the flooded sites had a higher average backscatter: −10.2 dB (unflooded) vs. −9.6 dB (flooded) in the marl prairie sites and −10.5 dB (unflooded) vs. −9.8 dB (flooded) in the cypress/pine sites.

Over the 25-month period of this study, radar backscatter measurements varied by a minimum of 4.4 dB (a factor of 2.8) to 9.0 dB (a factor of 8) in the different study sites. The range of backscatter measurements was equal for the both wooded and non-wooded sites. However, for the wooded sites, there was more seasonal variation in radar backscatter during non-flooded conditions than during flooded conditions. A similar pattern was observed in three of the marl prairie sites (Sites 3, 4, and 15) where the range is backscatter was higher during the dry season than during the wet season. However, in three other sites (Sites 7, 8, and 14), the variations during the wet and dry seasons were nearly identical. The lowest radar backscatter measurements were observed in the wet marsh site that experienced the deepest water depths (Sites 9 and 11).

A careful analysis of the water level, soil moisture, and precipitation in comparison to the ERS radar backscatter measurements does provide a better understanding for the sources of the variations observed in Fig. 8. Fig. 9 presents a plot of ERS backscatter as a function of soil moisture from the data collect in this study. This plot shows that when marl prairie sites are unflooded there is significant variation in radar backscatter that is correlated with soil moisture. The dependence of ERS radar backscatter on soil moisture variations is also evident through comparison of data collected during the two dry seasons that occurred during the study (October 1997 to April 1998 and October 1998 to April 1999). Fig. 10 presents a plot of ERS backscatter and water depth as function of time for two test sites: Site 7 (marl prairie) and Site 5 (cypress dome). Both of these sites were not flooded at the end of the dry seasons in both 1998 (May/July) and 1999 (April/May). However, the average ERS radar backscatter measurements at both sites were much lower in the dry season observations of 1999 than in 1998.

From Table 2, it can be seen that precipitation levels were much higher during the wet season of 1997/1998 than they were during the same period in 1998/1999. This variation in precipitation is reflected in the average water levels during the end of the dry season. The average water depth at Sites 1, and 3 to 8 in the period of March to May (end of the dry season) was 1.9 cm in 1998 compared 0.3 cm in 1999. These water depth data show that the unflooded sites had much less moisture during the March to May time period in 1999 than in 1998, and hence, should have lower soil moisture levels. Table 4 presents the average radar backscatter for all sites when they were unflooded during the March to May 1998 and 1999 time periods. On average, the radar backscatter at the end of the 1999 dry season was 5.4 dB lower than at the end of the 1998 dry season, with very little difference between non-wooded and wooded wetlands.

The above discussion highlights the importance of understanding the influence of soil moisture when analyzing temporal sequences of ERS backscatter and water depth measurements such as those presented in Fig. 10. When comparing the average backscatter measurements between the unflooded time periods during May 1998 and the flooded time periods immediately before and after, the average backscatter during the unflooded conditions is higher than during the flooded conditions. However, making the same comparison using data collected in April/May

Table 5
Summary of regressions coefficients for plots of ERS radar backscatter as a function of water depth for non-wooded and wooded study sites in the south Florida region

Site	n	Intercept	Slope	R^2	Significance ($p<$)
Marl prairie sites					
1	22	−8.5	−0.088	0.05	0.32
3	5	−11.6	0.199	0.55	0.15
4	12	−8.7	−0.094	0.32	0.06
7	16	−6.5	−0.333	0.78	0.001
8	15	−7.7	−0.127	0.08	0.34
14	6	−9.1	−0.243	0.70	0.04
15	6	−8.3	−0.146	0.30	0.27
All sites[a]	77	−7.9	−0.189	0.28	0.0001
Cypress/pine sites					
5	15	−9.2	−0.036	0.12	0.21
6	7	−9.6	−0.194	0.45	0.11
12	9	−8.7	−0.097	0.42	0.06
All sites	31	−9.3	−0.052	0.18	0.02

[a] Excluding site 3.

of 1999 results in the backscatter during the unflooded conditions being lower than during the flooded conditions.

This trend was observed in all study sites. In Table 4, we present the difference in average radar backscatter measurements between flooded and unflooded conditions for the different study sites. We calculated this difference in two ways. First, we calculated the average radar backscatter for each site when it was flooded during the periods of June 1997 through December 1998 and compared these to the average backscatter when the site was not flooded in March to May of 1998. Second, we calculated the average backscatter for the period of January 1998 through August of 1999 for each site when it was flooded and compared it to the average backscatter when the site was not flooded in

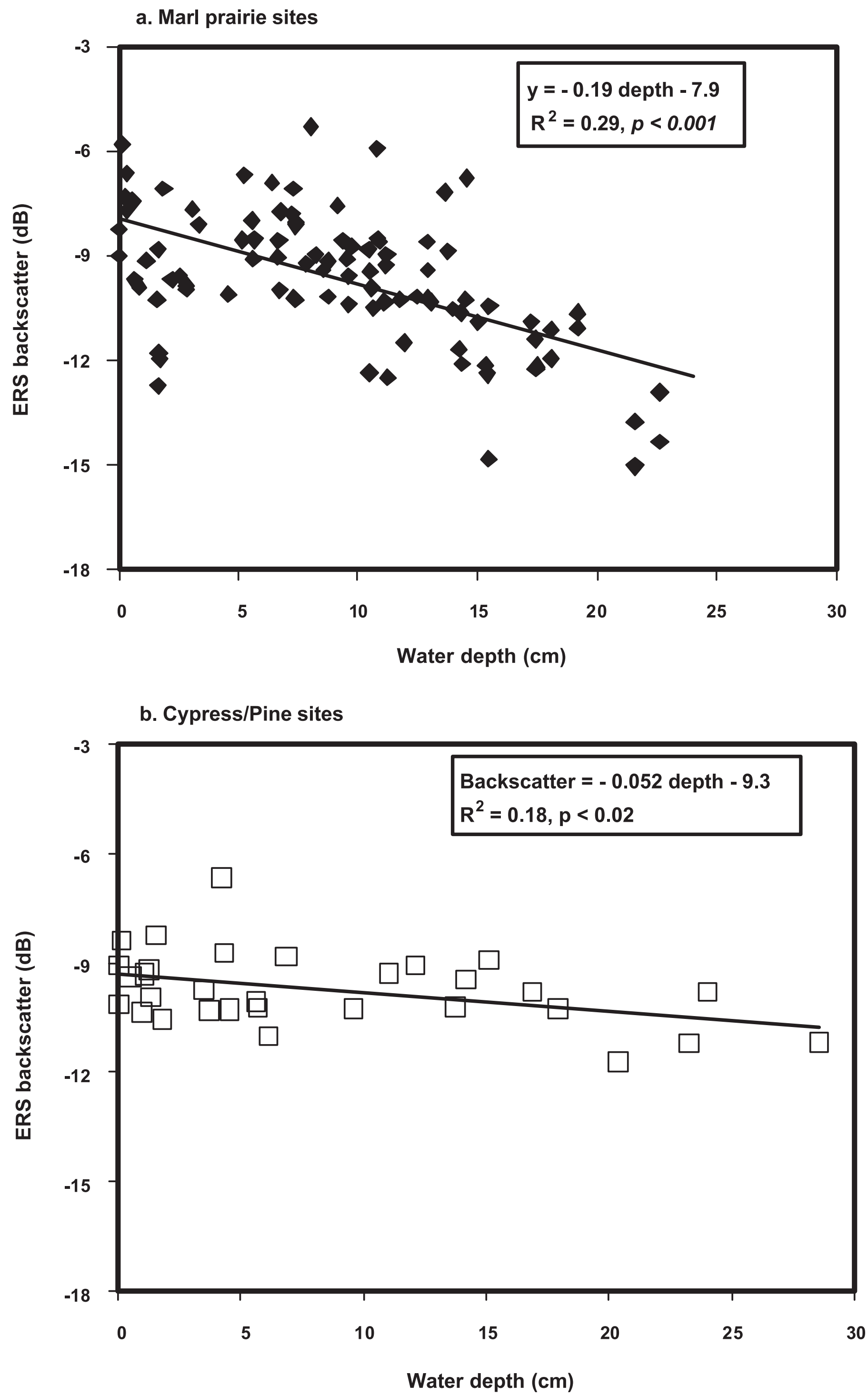

Fig. 12. Variation in ERS radar backscatter as a function of water depth in: (a) all marl prairie sites; and (b) all cypress and pine sites.

March to May of 1999. A positive difference in Table 4 means that the backscatter in the site increased when they became flooded, while a negative difference means the backscatter decreased when the sites became flooded.

The results in Table 4 are consistent in all sites. During the dry season of 1998 when the sites likely had high soil moisture, a flooding of the sites resulted in a 1.6-dB decrease in radar backscatter, with no difference occurring between wooded and non-wooded sites. During the dry season of 1999 (when the sites likely had lower soil moisture), they experienced a 3.3-dB increase in radar backscatter when they became flooded, with high increases being observed in the wooded wetlands. The observations support Hypothesis 1 of this study and the effects of flooding predicted by MIMICS (Fig. 3). We expect all the sites to have high soil moisture levels (similar to the conditions

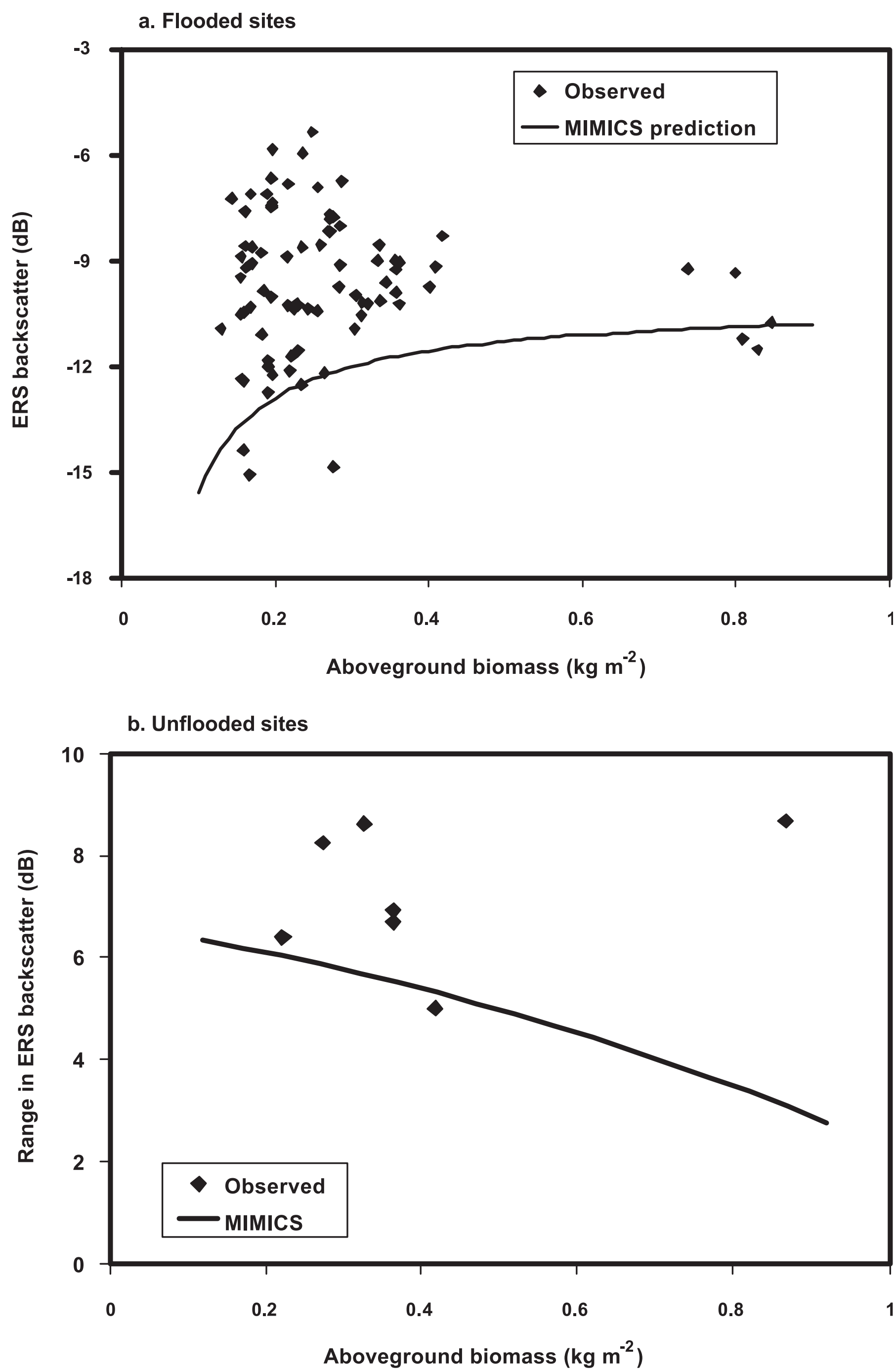

Fig. 13. Variation in ERS radar backscatter as a function of aboveground biomass: (a) backscatter as a function of biomass in all flooded marl prairie sites; (b) range in backscatter as a function of biomass in all non-flooded marl prairie sites.

observed in March–May 1998) prior to and immediately after flooding occurs. When flooding does occur, the data show there is a decrease in radar backscatter.

One clear trend present in the data from Site 7 in Fig. 10 is the strong inverse correlation between changes in water depth and changes in radar backscatter, e.g., as water depth increases, radar backscatter decreases. Although not as evident the same trend is also present in the data for Site 5. Fig. 11 presents a plot of ERS backscatter as a function of water depth for these two sites showing the correlation between these variables. Table 5 summarizes the regression equation of ERS backscatter as function of water depth for all sites. We can see that there is a positive relationship between these two variables for all sites except one. The one case where a positive slope occurs (Site 3) also had the highest aboveground biomass of any of the marl prairie sites. Fig. 12 presents a plot of ERS backscatter as function of water depth for all marl prairie (except Site 3) and all cypress/pine sites combined. These plots show that overall there is a statistically significant decrease in radar backscatter as water depth increases, which supports Hypothesis 3.

Finally, our analyses of the data indicate that variations in biomass had relatively little effect on the radar backscatter signature, and do not support either Hypothesis 4 or Hypothesis 5. If biomass had a strong influence on the microwave scattering signature, we would expect: (a) that radar backscatter in flooded sites would increase as biomass increases; and (b) the overall range in backscatter in the unflooded sites to be lowest in those sites with the highest biomass. Fig. 13a presents a plot of radar backscatter as a function of biomass for the flooded sites. In this plot, we reduced the average biomass of a plot (from Table 3), an amount proportional to the depth of the water at the time of data collection. In this plot, there is no apparent relationship between biomass and radar backscatter. According to theoretical models, the range in backscatter in unflooded sites should decrease as biomass increases. Fig. 13b shows this not to be the case for the sites in this study.

6. Discussion

In this study, we have demonstrated that variations in hydrologic conditions result in very large variations in radar backscatter from wetlands in southern Florida. During unflooded conditions, radar backscatter varies by a factor of 8 (9 dB) in both wooded and non-wooded wetlands. The same level of variation is observed in non-wooded wetlands when they are flooded, with lower levels of variation (5 dB) occurring in the wooded wetlands.

Variations in radar backscatter associated with changes in soil moisture and flooding predicted by the theoretical scattering model (MIMICS) were present in the ERS SAR data. Large variations in backscatter as a result of changes in soil moisture were clearly observed in the data. Variations in soil moisture during the dry seasons between two different periods were observed in all the study sites. Our interpretation is that all sites, there was a drop in radar backscatter when the sites became flooded. This reduction in backscatter occurred for all three major vegetation types: marl prairie, cypress, and pine flatwoods (Table 4). The magnitude of this drop for the marl prairie sites (1–2 dB), however, is much lower than the figure predicted by MIMICS. Finally, we did see a significant drop in radar backscatter as a function of increasing water depth, again for the major vegetation types (Figs. 11 and 12). The sensitivity to water depth was higher in the marl prairie sites than in the cypress/pine sites.

Our analyses indicates that variations in biomass had a relatively little impact on variations in backscatter associated with changes in soil moisture and water level. The vegetation of the sites used in this study had relatively short canopies, low biomass levels and small stem sizes; therefore, these should be viewed with certain degree of caution. In other studies where higher biomass levels occurred in the flooded sites, there was a strong influence of biomass on radar backscatter. For example, LeToan et al. (1997) noted a positive correlation in rice plant biomass and ERS backscatter; however, the maximum biomass level in LeToan et al. (1997) was 3.5 kg m^{-2}, which is 1 order-of-magnitude higher than the levels present in the sites in this study. Pope et al. (1997) concluded that wetlands with dense biomass and large stems experienced an increase in backscatter when flooded, while those with less dense vegetation and small stems experienced a decrease in backscatter when flooded (similar to the conclusion of this study). However, Pope et al. (1997) did not measure variations in soil moisture in their unflooded sites. Based on the results of the present study, it is not possible to attribute the results in Pope et al. (1997) entirely to differences in vegetation structure and density—variations in soil moisture likely played a role as well. It is clear that future studies must include steps to document vegetation biomass structure, density, and biomass as well as soil moisture to clearly document the role of each of these factors on variations in radar backscatter.

Examination of the ERS images in Figs. 1 and 7 show complex patterns of image intensity within individual regions not only between wet and dry seasons, but also between different years. For example, the fact that the region within Water Conservation Area 3A remains darker than the surrounding areas throughout the year is consistent with the fact that water is permanently stored in this basin. The region that is actually flooded within the Everglades National Park can clearly be delineated as dark regions in the ERS-1 SAR imagery. Variations in water levels in the Everglades are controlled through a combination of the patterns of water release from the Conservation Areas north of the Park and seasonal precipitation patterns. The spatially patchiness of seasonal flooding within the Big Cypress National is clearly seen on the ERS images. Note that the more extensive flooding during the wet seasons of 1997 is entirely consistent with the higher precipitation experienced during this time. Finally, the results of this study show that variations in image intensity during dry periods denotes not only the switch from a flooded to non-flooded state, but also variations in soil moisture.

In summary, the results of this study clearly demonstrate the unique capability for using C-band spaceborne imaging radar data for monitoring hydrologic conditions within wetland systems with lower levels of aboveground biomass. Although variations in aboveground biomass do influence the radar signature at individual sites, temporal variations in radar backscatter largely reflect variations in soil moisture and patterns of flooding in the wetlands of this region. Correct interpretation of the temporal variations in the radar signatures requires an understanding of how seasonal precipitation patterns influence patterns of soil moisture and inundation. Once these hydrologic patterns are established for a region, then changes in radar backscatter can be interpreted in terms of expected changes in soil moisture, flooding, and water level.

Acknowledgements

Support for this research was provided by the U.S. Environmental Protection Agency under Grant Number R825156-01-0. The research presented in this paper has not been subjected to review by EPA and therefore does not necessarily reflect their views, and no official endorsement should be inferred. The authors would like to thank the anonymous reviewers for their insightful and helpful comments.

References

Alsdorf, D. E., Melack, J. M., Dunne, T., Mertes, L. A. K., Hess, L. L., & Smith, L. C. (2000). Interferometric radar measurements of water level changes on the Amazon flood plain. *Nature*, *404*, 174–177.

Alsdorf, D. E., Smith, L. C., & Melack, J. M. (2001). Amazon floodplain water level changes measured with interferometric SIR-C radar. *IEEE Transactions on Geoscience and Remote Sensing*, *39*, 423–431.

Bourgeau-Chavez, L. L., Kasischke, E. S., Brunzell, S. M., Mudd, J. P., Smith, K. B., & Frick, A. L. (2001). Analysis of spaceborne SAR data for wetland mapping and flood monitoring in Virginia riparian ecosystems. *International Journal of Remote Sensing*, *22*, 3665–3687.

Bourgeau-Chavez, L. L., Kasischke, E. S., & Smith, K. B. (1996). Using satellite radar imagery to monitor flood conditions in wetland ecosystems of southern Florida. In G. Cecchi, G. D'Urso, E. T. Engman, & P. Gudmandsen (Eds.), *Remote sensing of vegetation and sea, vol. 2959* (pp. 139–148). Taormina, Italy: SPIE.

Brivio, P. A., Colombo, R., Maggi, M., & Tomasoni, R. (2002). Integration Remote sensing data and GIS for accurate mapping of flooded areas. *International Journal of Remote Sensing*, *23*, 429–441.

Brown, R. B., Stone, E. L., & Carlilse, V. W. (1990). Soils. In R. L. Ewel, & J. J. Ewel (Eds.), *Ecosystems of Florida* (pp. 35–69). Orlando, FL: University of Central Florida Press.

Dobson, M. C., Ulaby, F. T., & Pierce, L. E. (1995). Land-cover classification and estimation of terrain attributes using synthetic-aperture radar. *Remote Sensing of Environment*, *51*, 199–214.

Duever, M. J., Carlson, J. E., Meeder, J. F., Duever, L. C., Gunderson, L. H., Riopelle, L. A., Alexander, T. R., Meyers, R. L., & Spangler, D. P. (1986). *The Big Cypress National Preserve*. Naples, FL: National Audubon Society.

Duever, M. J., Meeder, J. F., Meeder, L. C., & McCollom, J. M. (1994). The climate of south Florida and its role in shaping the Everglades. In S. M. Davis, & J. C. Ogden (Eds.), *Everglades—the ecosystem and its restoration* (pp. 225–248). Delray Beach, FL: St. Lucie Press.

Dwivedi, R. S., Rao, B. R. M., & Bhattacharya, S. (1999). Mapping wetlands of the Sundaban Delta and its environs using ERS-1 SAR data. *International Journal of Remote Sensing*, *20*, 2235–2247.

Engheta, N., & Elachi, C. (1982). Radar scattering from a diffuse vegetation layer over a smooth surface. *IEEE Transactions on Geoscience and Remote Sensing*, *20*, 212–216.

Gunderson, L. H. (1994). Vegetation of the Everglades: Determinants of species composition. In S. M. Davis, & J. C. Ogden (Eds.), *Everglades—The ecosystem and its restoration* (pp. 323–340). Delray Beach, FL: St. Lucie Press.

Hess, L. L., Melack, J. M., Filoso, S., & Wang, Y. (1995). Delineation of inundated area and vegetation along the Amazon floodplain with the SIR-C synthetic aperture radar. *IEEE Transactions on Geoscience and Remote Sensing*, *33*, 896–904.

Hess, L. L., Melack, J. M., & Simonett, D. S. (1990). Radar detection of flooding beneath the forest canopy: A review. *International Journal of Remote Sensing*, *11*, 1313–1325.

Imhoff, M. L., Vermillion, C., Story, M. H., Choudhury, A. M., Gafoor, A., & Polcyn, F. (1987). Monsoon flood boundary delineation and damage assessment using space borne imaging radar and Landsat data. *Photogrammetric Engineering and Remote Sensing*, *53*, 405–413.

Kandus, P., Karszenbaum, H., Pultz, T., Parmuchi, G., & Bava, J. (2001). Influence of flood conditions and vegetation status on the radar backscatter of wetland ecosystems. *Canadian Journal of Remote Sensing*, *27*, 651–662.

Kasischke, E. S., & Bourgeau-Chavez, L. L. (1997). Monitoring south Florida wetlands using ERS-1 SAR imagery. *Photogrammetric Engineering and Remote Sensing*, *33*, 281–291.

Kasischke, E. S., Bourgeau-Chavez, L. L., Smith, K. B., Romanowicz, E., & Richardson, C. J. (1997). Monitoring hydropatterns in southern Florida ecosystems using ERS SAR data. *Proceedings of the 3rd ERS symposium on space in service of our environment* (pp. 71–76). Florence, Italy: European Space Agency.

Krohn, M. D., Milton, N. M., & Segal, D. B. (1983). Seasat synthetic aperture radar (Sar) response to lowland vegetation types in eastern Maryland and Virginia. *Journal of Geophysical Research*, *88*, 1937–1952.

Kurosu, T., Masaharu, F., & Chiba, K. (1995). Monitoring of rice crop growth from space using the ERS-1 C-band SAR. *IEEE Transactions on Geoscience and Remote Sensing*, *33*, 1092–1096.

LeToan, T., Ribbes, F., Wang, L. F., Floury, N., Ding, K. H., Kong, J. A., Fujita, M., & Kurosu, T. (1997). Rice crop mapping and monitoring using ERS-1 data based on experiment and modeling results. *IEEE Transactions on Geoscience and Remote Sensing*, *35*, 41–56.

Liew, S. C., Kam, S. P., Tuong, T. P., Chen, P., Minh, V. Q., & Lim, H. (1998). Application of multitemporal ERS-2 synthetic aperture radar in delineating rice cropping systems in the Mekong River Delta, Vietnam. *IEEE Transactions on Geoscience and Remote Sensing*, *36*, 1412–1420.

Meadows, P. J., Laur, H., & Shattler, B. (1999). The calibration of ERS SAR imagery for land applications. *Earth Observation Quarterly*, *62*, 5–9.

Moreau, S., & Le Toan, T. (2003). Biomass quantification of Andean wetland forages using ERS satellite SAR data for optimizing livestock management. *Remote Sensing of Environment*, *84*, 477–492.

Morrissey, L. A., Durden, S. L., Livingston, G. P., Stearn, J. A., & Guild, L. S. (1996). Differentiating methane source areas in arctic environments with multitemporal ERS-1 SAR data. *IEEE Transactions on Geoscience and Remote Sensing*, *34*, 667–673.

Morrissey, L. A., Livingston, G. P., & Durden, S. L. (1994). Use of SAR in regional methane exchange studies. *International Journal of Remote Sensing*, *15*, 1337–1342.

Ormsby, J. P., Blanchard, B. J., & Blanchard, A. J. (1985). Detection of lowland flooding using active microwave systems. *Photogrammetric Engineering and Remote Sensing*, *51*, 317–328.

Panigrahy, S., Chakraborty, M., Sharma, S. A., Kundu, N., Ghose, S. C., & Pal, M. (1997). Early estimation of rice area using temporal ERS-1 synthetic aperture radar data—A case study for the Howrah and Hughly districts of West Bengal, India. *International Journal of Remote Sensing*, *18*, 1827–1833.

Parmuchi, M. G., Karszenbaum, H., & Kandus, P. (2002). Mapping wetlands using multi-temporal RADARSAT-1 data and a decision-based classifier. *Canadian Journal of Remote Sensing*, *28*, 175–186.

Pope, K. O., Rejmankova, E., & Paris, J. F. (2001). Spaceborne imaging radar-C (SIR-C) observations of groundwater discharge and wetlands associated with the Chicxulub impact crater, northwestern Yucatan Peninsula, Mexico. *Geological Society of America Bulletin*, *113*, 403–416.

Pope, K. O., Rejmankova, E., Paris, J. F., & Woodruff, R. (1997). Detecting seasonal flooding cycles in marshes of the Yucatan Peninsula with SIR-C polarimetric radar imagery. *Remote Sensing of Environment*, *59*, 157–166.

Ramsey, E. W. (1995). Monitoring flooding in coastal wetlands by using radar imagery and ground-based measurements. *International Journal of Remote Sensing*, *16*, 2495–2502.

Ramsey, E. W., Nelson, G. A., Laine, S. C., Kirkman, R. G., & Topham, W. (1997). Generation of coastal marsh topography with radar and ground-based measurements. *Journal of Coastal Research*, *13*, 1335–1342.

Rao, B. R. M., Dwivedi, R. S., Kushwaha, S. P. S., Bhattacharya, S. N., Anand, J. B., & Dasgupta, S. (1999). Monitoring the spatial extent of coastal wetlands using ERS-1 SAR data. *International Journal of Remote Sensing*, *20*, 2509–2517.

Ribbes, F., & Le Toan, T. (1999). Rice field mapping and monitoring with RADARSAT data. *International Journal of Remote Sensing*, *20*, 745–765.

Rio, J. N. R., & Lozano-Garcia, D. F. (2000). Spatial filtering of radar data (RADARSAT) for wetlands (brackish marshes) classification. *Remote Sensing of Environment*, *73*, 143–151.

Rosenqvist, A. (1999). Temporal and spatial characteristics of irrigated rice in JERS-1 L-band SAR data. *International Journal of Remote Sensing*, *20*, 1567–1587.

Rosenqvist, A., & Birkett, C. M. (2002). Evaluation of JERS-1 SAR mosaics for hydrological applications in the Congo River basin. *International Journal of Remote Sensing*, *23*, 1283–1302.

Rosenqvist, A., Forsberg, B. R., Pimentel, T., Rauste, Y. A., & Richey, J. E. (2002). The use of spaceborne radar data to model inundation patterns and trace gas emissions in the central Amazon floodplain. *International Journal of Remote Sensing*, *23*, 1303–1328.

Shao, Y., Fan, X. T., Liu, H., Xiao, J. H., Ross, S., Brisco, B., Brown, R., & Staples, G. (2001). Rice monitoring and production estimation using multitemporal RADARSAT. *Remote Sensing of Environment*, *76*, 310–325.

Tanis, F. J., Bourgeau-Chavez, L. L., & Dobson, M. D. (1994). Application of ERS-1 SAR for coastal inundation. *1994 IEEE Geosci. Remote Sens. Society* (pp. 1481–1483). Pasadena, CA: IEEE.

Townsend, P. A. (2001). Mapping seasonal flooding in forested wetlands using multi-temporal Radarsat SAR. *Photogrammetric Engineering and Remote Sensing*, *67*, 857–864.

Townsend, P. A. (2002). Relationships between forest structure and the detection of flood inundation in forested wetlands using C-band SAR. *International Journal of Remote Sensing*, *23*, 443–460.

Townsend, P. A., & Foster, J. R. (2002). A synthetic aperture radar-based model to assess historical changes in lowland floodplain hydroperiod. *Water Resources Research*, *38* (art. no.-1115).

Townsend, P. A., & Walsh, S. J. (1998). Modeling floodplain inundation using an integrated GIS with radar and optical remote sensing. *Geomorphology*, *21*, 295–312.

Ulaby, F. T., Moore, R. K., & Fung, A. K. (1982). *Microwave remote sensing, active and passive: Volume II. Radar remote sensing and surface scattering and emission theory.* Reading, MA: Addison-Wesley Publishing, 607 pp.

Ulaby, F. T., Sarabandi, K., McDonald, K., & Dobson, M. C. (1990). Michigan microwave canopy scattering model (MIMICS). *International Journal of Remote Sensing*, *11*, 1223–1253.

Werle, D., Martin, T. C., & Hasan, K. (2000). Flood and coastal zone monitoring in Bangladesh with Radarsat ScanSAR: Technical experience and institutional challenges. *Johns Hopkins APL Technical Digest*, *21*, 148–154.

Zhou, C. H., Luo, J. C., Yang, C. J., Li, B. L., & Wang, S. L. (2000). Flood monitoring using multi-temporal AVHRR and RADARSAT imagery. *Photogrammetric Engineering and Remote Sensing*, *66*, 633–638.